(2)

STUDY OF THE INFLUENCE OF METALLURGICAL FACTORS ON FATIGUE AND FRACTURE OF AEROSPACE STRUCTURAL MATERIALS

by
James Lankford
David L. Davidson
Gerald R. Leverant
Kwai S.Chan

AFOSR FINAL REPORT

This research was sponsored by the Air Force Office of Scientific Research,
Electronic and Materials Sciences Directorate
Under Contract F49620-83-C-0054
Approved for release; distribution unlimited.

February 1986

SOUTHWEST RESEARCH INSTITUTE
SAN ANTONIO HOUSTON

SOUTHWEST RESEARCH INSTITUTE
Post Office Drawer 28510, 6220 Culebra Road
San Antonio, Texas 78284

STUDY OF THE INFLUENCE OF METALLURGICAL FACTORS ON FATIGUE AND FRACTURE OF AEROSPACE STRUCTURAL MATERIALS

by
James Lankford
David L. Davidson
Gerald R. Leverant
Kwai S. Chan

AFOSR FINAL REPORT

This research was sponsored by the Air Force Office of Scientific Research,
Electronic and Materials Sciences Directorate
Under Contract F49620-83-C-0054
Approved for release; distribution unlimited.

February 1986

Approved:

U. S. Lindholm, Vice President
Engineering and Materials Sciences Division

UNCLASSIFIED

SECURITY CLASSIFICATION OF THIS PAGE *(When Data Entered)*

REPORT DOCUMENTATION PAGE		READ INSTRUCTIONS BEFORE COMPLETING FORM
1. REPORT NUMBER AFOSR-TR- 86-0493	2. GOVT ACCESSION NO. AD-A170218	3. RECIPIENT'S CATALOG NUMBER
4. TITLE *(and Subtitle)* Study of the Influence of Metallurgical Factors on Fatigue and Fracture of Aerospace Structural Materials		5. TYPE OF REPORT & PERIOD COVERED Final Scientific Report 1 Jan 1983 - 31 Dec 1985
		6. PERFORMING ORG. REPORT NUMBER ~~06-7436~~ SWRI-7436
7. AUTHOR(s) James Lankford, Gerald R. Leverant David L. Davidson, Kwai S. Chan		8. CONTRACT OR GRANT NUMBER(s) F49620-83-C-0054
9. PERFORMING ORGANIZATION NAME AND ADDRESS Southwest Research Institute 6220 Culebra Road (P.O. Drawer 28510) San Antonio, TX 78284		10. PROGRAM ELEMENT, PROJECT, TASK AREA & WORK UNIT NUMBERS 61102F 2306/A1
11. CONTROLLING OFFICE NAME AND ADDRESS Air Force Office of Scientific Research Bolling AFB, Building 410 Washington, DC 20332		12. REPORT DATE February 1986 13. NUMBER OF PAGES 27
14. MONITORING AGENCY NAME & ADDRESS*(if different from Controlling Office)*		15. SECURITY CLASS. *(of this report)* Unclassified 15a. DECLASSIFICATION/DOWNGRADING SCHEDULE

16. DISTRIBUTION STATEMENT *(of this Report)*

Approved for public release; distribution unlimited.

17. DISTRIBUTION STATEMENT *(of the abstract entered in Block 20, if different from Report)*

18. SUPPLEMENTARY NOTES

19. KEY WORDS *(Continue on reverse side if necessary and identify by block number)*

Fatigue
Fracture
Crack Growth
Nickel-Base Superalloys
Aluminum Alloys
Titanium Alloys
Single Crystals
Crack Tip Plasticity
Crack Growth Modeling
Crystallographic Orientation

20. ABSTRACT *(Continue on reverse side if necessary and identify by block number)*

This report summarizes the results of a two-phase study involving (1) experimental characterization and analytical modeling of fatigue crack tip micromechanics in aerospace structural (Al and Ti) alloys, and (2) identification and modeling of key factors controlling subcritical crack growth and unstable fracture in single crystal nickel-base superalloys.

(continued)

DD FORM 1473 JAN 73 86 7 23 1

UNCLASSIFIED

SECURITY CLASSIFICATION OF THIS PAGE *(When Data Entered)*

Fatigue crack growth at near-threshold rates has been modeled using microstructurally-controlled micromechanical crack tip parameters. The model is based on the concept of crack opening by means of local slip lines whose length and dislocation density are controlled by the alloy microstructure. Crack tip opening displacement, crack tip strain, and the increment of crack advance are micromechanical parameters which depend on the number, spacing, and orientation of the slip lines. The model relates all of these prameters, and can be used to predict the increment of crack advance if the microstructure-dependent slip line length is known. Crack tip micromechanics information obtained using a cyclic loading stage within the SEM is used to provide input data and correlating results for two aluminum alloys and a titanium alloy. The slip line length required (predicted) by the model was found to roughly equal the dispersoid spacing for the Al alloys, and the grain size in the Ti alloy.

Fatigue crack growth mechanisms in Ni-base superalloy single crystals were examined as a function of crystallographic orientation, stress state and slip character. Using compact-tension and tubular specimens, fatigue crack growth in Mar-M200 single crystals of various crystallographic orientations was determined in both unidirectional and multiaxial cyclic loads, at temperatures where the slip character was either localized (25 C) or homogeneous (980 C). In most cases, subcritical crack growth at ambient temperature occurred along crystallographic planes with crack deflection, branching and roughness-induced closure present in some specimens. The apparent effects of crystallographic orientation and stress state were shown to be the consequence of roughness-induced crack closure. On the other hand, crack growth at 982 C under both uniaxial and multiaxial fatigue were shown to occur in a non-crystallographic manner with the fracture surfaces generally exhibiting striations. It was shown that in the absence of roughness-induced closure, an effective ΔK that accounted for mixed-mode loading and elastic anisotropy represented the driving force for crack growth in both uniaxial and multiaxial fatigue at ambient and elevated temperatures. The crack growth rates, uniquely defined in terms of the effective ΔK were independent of the applied stress state and crystallographic orientation. Furthermore, it was shown that the change in fracture mechanism from crystallographic cracking at 25 C to non-crystallographic cracking at 982 C was due to the propensity for homogeneous multiple slip at the crack tip at 982 C. The overall fatigue mechanism in Mar-M200 single crystals was examined by extending a fracture model to consider the crack-tip slip behavior that led to cracking along crystallographic planes.

FOREWORD

This report summarizes work carried out under a three-year program to investigate key problems associated with the fatigue of aerospace structural materials, and with the fatigue and fracture of advanced engine alloys. The program was divided into two tasks, the first dealing with aluminum and titanium airframe alloys, the second with nickel-base single crystal superalloys.

The structural alloy task was focused upon the questions of how fatigue cracks actually extend, how the process can be described in micromechanical terms, and whether it might be possible to incorporate the latter into a microstructure-dependent model. Until recently, addressing the first two questions has been virtually impossible. However, the development of the SEM cyclic loading stage, and an associated technique (stereoimaging strain analysis) for quantifying crack tip yielding, have provided unique opportunities to determine factors heretofore the domain of assumption and rather simple-minded approximation. With these new capabilities, it has become possible to quantify crack tip opening, strains, local stress-strain failure laws, and cyclic microfracture development, within a region no more than a few micrometers from the crack tip. This report describes how such observations have been used as the basis for a physically realistic crack growth law, and how the latter has been validated for several microstructurally-different alloys.

Ni-base single crystal alloys are attractive materials for turbine engine applications because of improved creep resistance, good thermal fatigue behavior, and high incipient melting point. These beneficial properties can lead to more efficient turbine engines by allowing significant increases in engine temperature and blade stress. The efficient and safe utilization of Ni-base single crystal alloys for advanced engine applications also requires knowledge of the crack growth response and the fundamental fracture mechanisms of these anisotropic materials under complex stress histories. The focus of Task II has been to examine the effects of crystallographic orientation, stress state, and slip character on the mode of cracking and the subcritical crack growth resistance of a Ni-base single crystal alloy. The results of this work have provided a better understanding of fatigue processes in Ni-base single crystals at ambient and elevated temperatures, as well as a methodology for correlating multiaxial fatigue crack growth.

LIST OF ILLUSTRATIONS

Task 1. Influence of Metallurgical Structure Upon Crack Tip Micromechanics

Task 2. Fracture Mechanisms in Single Crystal Nickel-Base Superalloys

TABLE OF CONTENTS

LIST OF ILLUSTRATIONS (CONTINUED)

I. INFLUENCE OF METALLURGICAL STRUCTURE UPON CRACK TIP MICROMECHANICS

A. Research Objectives

1. Define experimentally the physical basis and extent of crack advance in alloys of varying, well-characterized microstructure.

2. Determine and measure experimentally the microstructural and micromechanical elements which control subcritical crack advance.

3. Incorporate microstructural and crack tip micromechanical parameters into a quantitative, fundamentally valid crack growth model.

4. Evaluate the crack growth model by using it to predict crack advance parameters in alloys of varying microstructure and chemical makeup.

B. Summary of Research Efforts

1. Development of a Physically Valid Crack Growth Rate Model

Based on work [1,2] performed under the preceding AFOSR contract, it was clear that the growth of fatigue cracks in structural alloys could be modeled by allowing a crack tip element to fail by a low cycle fatigue process. However, of the various models in the literature [3-7] which attempt to treat crack advance in this way, all involve extensive assumptions. In brief, these models generally require as input the local cyclic crack tip strain, crack tip opening displacement, the relevant low cycle failure law, the distance over which damage is accumulating, and the stress-cyclic strain relationship. Usually only the latter is known; the remaining values are assumed, as for example [5,6], that the macroscopically derived low cycle fatigue relationship can be used to describe failure of a crack tip ligament. However, the development under AFOSR-sponsorship of the technique of stereo-imaging strain analysis has permitted, for the first time, direct, quantitative measurement of localized crack tip parameters. The approach is described in detail elsewhere [8,9]; it involves using photogrammetry equipment to measure displacements around the tips of cracks loaded in a servo-controlled cyclic loading stage [10] inside the SEM.

Early in the current program, fatigue crack tip parameters in 7075-T651 (ingot) and 7091 (P/M) aluminum alloys were carefully characterized [11] using these procedures. As a result, it was found that the measured crack tip opening displacements (CTOD), maximum strain at the crack tip ($\Delta\varepsilon_p$), and the crack extension increments (Δa) could be correlated with the effective cyclic stress intensity ΔK_{eff} by

$$CTOD = C\Delta K_{eff}^{q}$$

$$\Delta\varepsilon_p = K_o\ \Delta K_{eff}^{r}$$

$$\Delta a = A_o\ \Delta K_{eff}^{n}$$

where q, r, n, C, K_o, and A_o are constants. In addition, the crack tip low cycle fatigue law was determined, whereby incremental failure of material required ΔN cycles according to

$$\Delta\varepsilon_p\ \Delta N^{\beta} = \varepsilon_c$$

where β is a constant (not necessarily equal to the macroscopic low cycle fatigue exponent), and ε_c is the cumulative critical (local) crack tip strain when the crack extends, which corresponds to the creation of a single striation. Extensive numerical data for all these parameters as functions of ΔK_{eff} were obtained, and analyzed in detail.

More importantly, the general behavior of these parameters has been incorporated into a model [12] for crack advance, based on the crack tip geometry shown in Figure 1. The tip is considered to deform by emitting a number of slip lines N(K) at an angle θ to the line of the crack; the higher the applied stress intensity (K), the greater is the number of slip lines. Direct observation [13] of crack opening and closing within the SEM verifies this basic process.

Using the crack tip geometry shown in Figure 1,

$$CTOD_x = N(K)\ D_n b \sin\theta$$

where $D_n b$ is the displacement per slip line. Here, D_n is the difference between the number of dislocations which are emitted during the loading of a crack tip, and those which move back into the tip upon unloading; b is the Burgers vector. The associated crack growth increment, taken on average perpendicular to the loading, is

$$\Delta a = N(K) D_n b \cos\theta$$

The length of the slip lines r_s, the number of dislocations on the slip plane D_n, and the applied stress can all be related through the mathematics of a dislocation pileup, whereby [14]

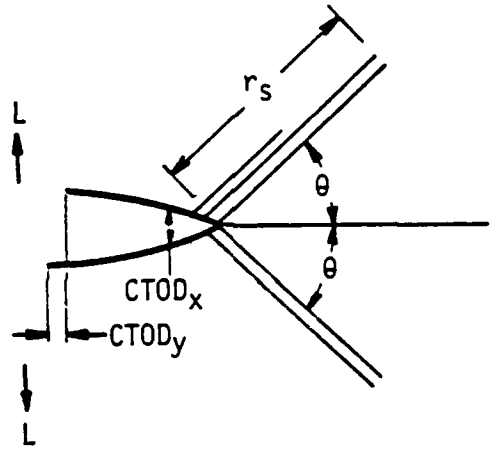

Figure 1. Crack opening geometry induced by load L. Crack tip opening displacement (CTOD) arises from dislocation activity on slip lines inclined at angle θ to the direction of crack growth. Individual slip line length is limited to r_s by microstructural obstacles.

$$D_n b = \frac{\pi(1-\nu)}{\mu} \tau r_s$$

where ν = Poissons ratio, μ = the shear modulus, and τ = the shear stress on the slip plane. Shear stress on the slip plane is determined from the cyclic stress-strain curve

$$\Delta\tau = K_1 \left(\frac{\Delta\varepsilon_p}{2}\right)^{n'}$$

where K_1 and n' are constants.

Combining all of these relationships, it is possible to write the crack growth rate as

$$\frac{da}{dN} = \frac{\Delta a}{\Delta N} = \frac{N(K)C \cos\theta\, r_s}{(\varepsilon_c/K_o)^{1/\beta}} \Delta K_{eff}^{(n'+1/\beta)r}$$

where C combines a number of constants given in the above equations. The result is a quantitative, microstructure-sensitive, micromechanical model for fatigue crack growth which incorporates measured crack tip parameters and observed crack advance mechanisms. Evaluation can be accomplished in several ways, all of which involve assumptions regarding one or more of the unknown (but physically defined) parameters in the model.

The model is summarized in condensed form in Figure 2. Typical crack tip strains ($\Delta\varepsilon_p$ corresponds to x, y = 0), the dependence of r_s upon microstructure, and striations (ss = Δa) are shown. These, together with the low cycle fatigue and cyclic stress-strain properties, provide analytical input. Actually, the evaluation of the model has proceeded in two ways, as shown: (I) measured CTOD, $\Delta\varepsilon_p$, ss, and LCF and cyclic σ-ε properties, are input to predict $^{da}/_{dN}$ as a function of ΔK, and the average (blocked) slip band length r_s; (II) measured CTOD and $\Delta\varepsilon_p$, LCF and cyclic σ-ε, and the slip line length r_s, are input to predict striation spacing and $^{da}/_{dN}$ versus ΔK. Exercise of the model in this way was one of the major efforts made during the research.

2. Evaluation of Model

Crack tip data for evaluating the model were generated for the following alloys:

7075-T651 (ingot) [11]
7091-T7E69 (P/M) [11]
Ti-6Al-4V (RA) (ingot) [16]

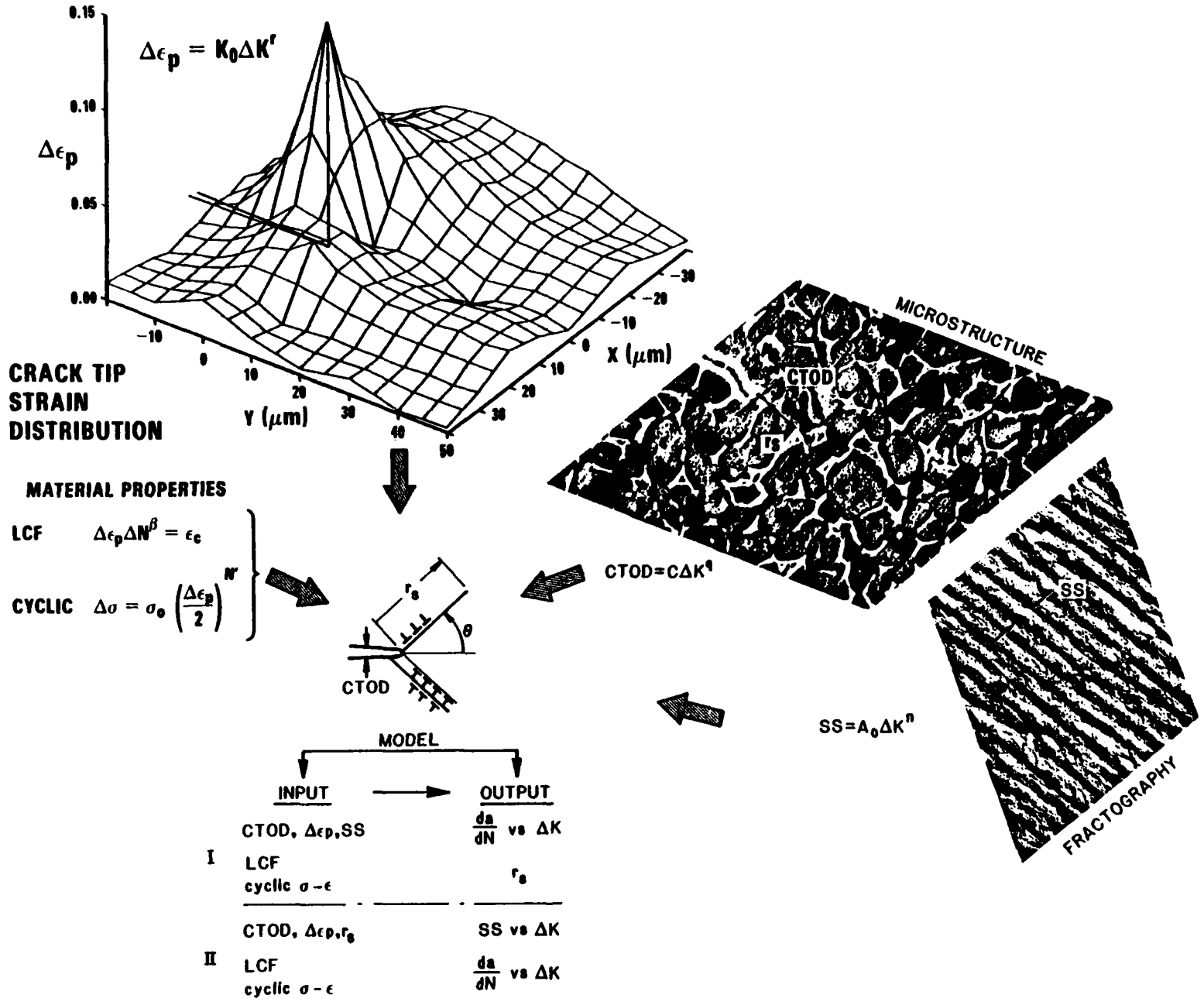

Figure 2. Crack tip geometric model integrating both microstructure and crack tip micromechanics.

Results were obtained in both vacuum and moist air environments over a stress intensity range of 4-12 $MN/m^{3/2}$.

For the aluminum alloys, the model was used in the first way, (I, Fig. 2), which inputs CTOD, crack tip strain and striation spacing, and outputs the slip distance. Optical, SEM, and transmission electron microscopy were used to evaluate the microstructure [15]. Correlation was found between the slip distance, derived using the model, and the mean free path between dispersoids, for both alloys. Table 1 summarizes these results. It is clear that the fabrication technique (ingot vs powder metallurgy), despite the attendant large difference in grain size, has had little effect on the results, a fact which further implicates dispersoid spacing as the likely controlling metallurgical parameter.

For the titanium alloy, the model was used in the second way (II, Fig. 2) in which CTOD, crack tip strain and the slip line length r_s were input, and the output was striation spacing. The controlling metallurgical factor was assumed to be the alpha grain size, since this structure has no precipitates or dispersoids. Table 2 compares the derived and measured striation spacings. The generally good agreement indicates that the alpha grain size is very likely to be the controlling microstructural parameter.

Our assessment of these studies is that the model gives useful results, even though it is not yet possible to predict crack growth rates without first measuring crack tip parameters. The model is, however, able to bring together in a physically realistic way the numerous factors affecting crack growth, and some of the microstructural parameters which influence it. The above evaluation indicates that the main hypotheses used in the model are roughly correct. Unfortunately, the model does not address directly the mechanism by which the microstructure at the tip of the crack is broken down during the crack growth process. Rather, it treats the tiny element being broken as a small specimen failing by low-cycle fatigue.

The experimental crack tip measurements, combined with the model, have helped to focus further work directed at:

- o analytical prediction of crack tip opening displacement and strain

and

- o the mechanism of lengthening.

3. Mechanism of Crack Advance

Dynamic observation of crack growth in the SEM loading stage has established [17] that for near threshold conditions, (1) crack advance is incremental and about equal to the striation spacing; (2) an increment of growth requires a finite number of cycles; (3) striation spacing is significantly greater than the average macroscopic crack growth rate. Further

TABLE 1

ALUMINUM ALLOYS
Slip Distances Derived Using the Geometric Crack Tip Model

Alloy	Environment	Slip Distance (μm) ± 2 μm	MFP Through Dispersoids (μm)
7075-T651	Vacuum	7.2	3.7-5
7075-T651	Moist Air	5.0	
7091	Vacuum	5.1	4.6-7.5
7091	Moist Air	6.9	

TABLE 2

Ti-6Al-4V TITANIUM ALLOY

Environment	Striation Spacing (μm)	
	Predicted	Measured
Vacuum	.09	0.1 (approximate)
Moist Air	.131	0.133

evidence for the mechanism by which the crack lengthens has been found by examining the crack tip on each loading cycle under very high resolution conditions in the SEM, using the cyclic loading stage.

The general process by which the crack lengthens has been determined, and is summarized in Table 3 and Figure 3. While the crack does not follow this pattern for every growth increment, the events listed in the table are most frequently observed.

The observed sequence of events accompanying growth also seems to fit with the formation of striations. Nix and Flower [18] have investigated striations by using SEM and STEM on thin foils which include the fracture surface. Their finding that a striation has two parts, one generating numerous dislocations and the other generating few dislocations, correlates very well with our observations of the crack growth process.

Using the observations described above, a hypothesis (Table 4) for the steps involved in the cyclic breakdown of the microstructure has been formulated. Some aspects of this hypothesis have been verified, but others remain to be tested. Although the hypothesis has been formulated for aluminum alloys, it may also be applicable to certain titanium alloy microstructures.

TABLE 3

STEPS IN FATIGUE CRACK LENGTHENING
(Near Threshold Stress Intensity)

Step	
1	Through cycling, an intense zone of tensile and shear strains is formed ahead of the crack tip.
2	Upon each unloading, the slip reverses (or nearly so).
3	Further cycling increases the tensile strain and CTOD, and a dominant slip line forms in the region of largest <u>combined</u> shear and tensile strain.
4	Tensile strain becomes discontinuous across the slip line, i.e., greater on one side than on the other.
5	The slip line begins to break, forming an extension to the crack. Multiple cycles may be required to increase crack length to the full extent of the slip line.

A striation is formed by the above process.

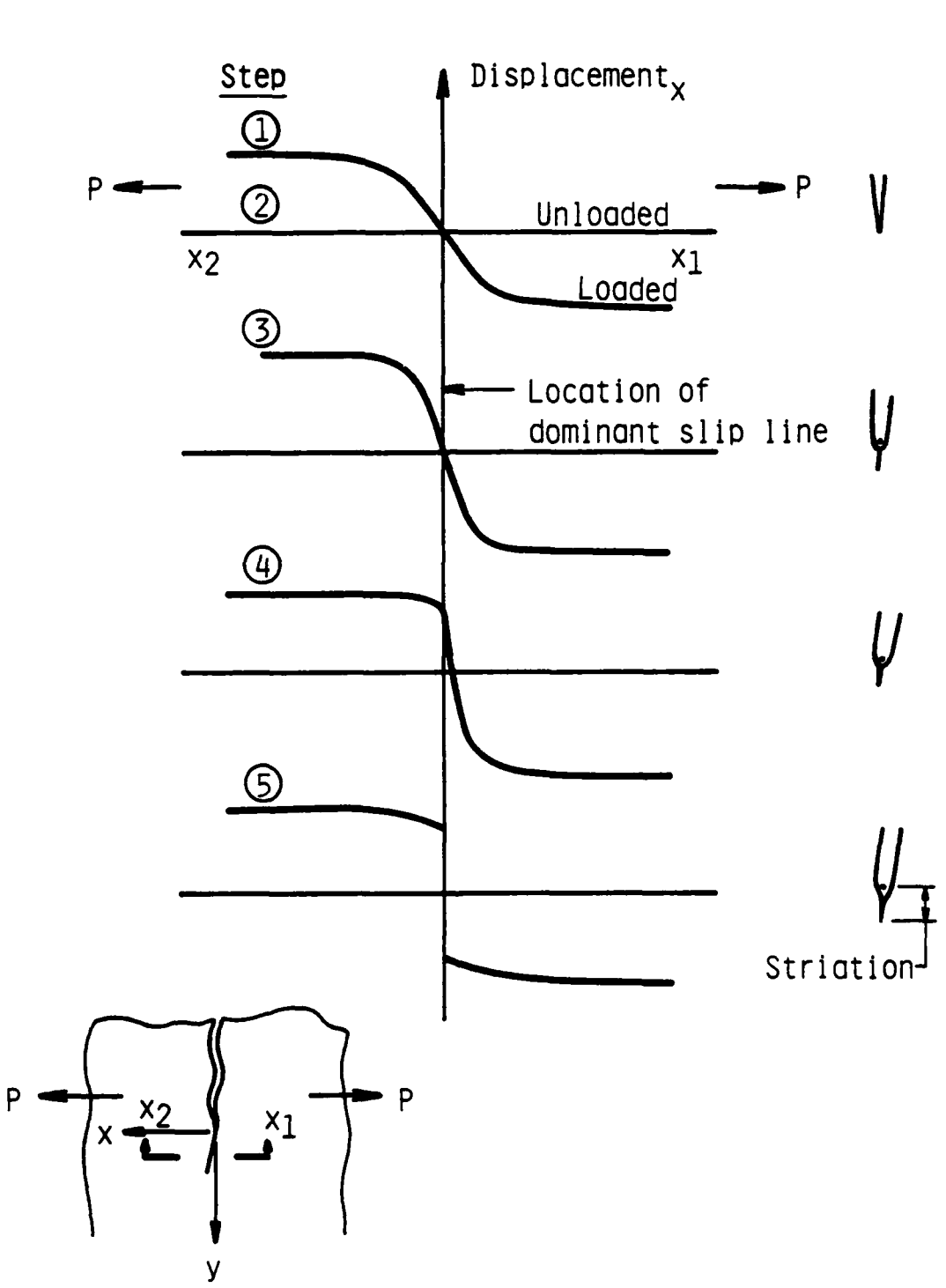

Figure 3. A schematic representation of displacements in the loading direction just ahead of the crack tip for each step in the sequence of crack growth listed in Table 3. As shown on the right of the figure, these steps lead to crack tip blunting, dominant slip line formation and striation formation.

TABLE 4

MICROSTRUCTURAL BREAKDOWN AT FATIGUE CRACK TIP (Hypothesis)

Presently applicable only to aluminum alloys

Step	
1	Dislocations are created and move away from the sharp crack tip on numerous slip planes as the cyclic load is increased.
2	Dislocations move back towards the crack tip during the unloading part of the cycle. Slip is multiple, but reversibility is not perfect.
3	Further cycling increasingly blunts the crack, tip and the strain just ahead of the tip increases. Slip ceases being homogeneous with the creation of a dominant slip line, which forms in the region of maximum combined shear strain and tensile stress. Inhomogeneous flow is caused by a large increase in dislocation density in the highly strained region, which makes slip increasingly difficult. Thus, slip concentrates on only the most highly stressed line, whose length is controlled by the distance to a microstructural barrier, or to a region of lower stress.
4	The slip line breaks due to the large local dislocation density, which decreases cohesive forces along the line, allowing the high tensile stresses in this region to pull the material apart.
5	Separation along the slip line requires several cycles, and results in a sharp crack tip with homogeneous deformation ahead of it.

The above process forms one striation consisting of two parts:

a) that due to crack tip blunting, and

b) that due to slip line microfracture.

C. Accomplishments

- o A crack tip slip line model has been developed which is used in conjunction with micromechanical crack tip deformation measurements and observation to predict crack extension increments.

- o Stereoimaging strain analysis and dynamic observation of crack tips within the SEM were used to determine the parameters required for a physically correct analysis, i.e., crack tip strain within 1 μm of the crack tip, crack tip slip line angle, and the relevant low cycle fatigue failure law for the tip, for several metal alloys.

- o Results of crack tip measurements for 7075-T651 ingot, 7091 P/M, and Ti-6Al-4V ingot alloys were used as input data in the model.

- o Crack extension increments were predicted with good accuracy; values for slip line length assumed as input parameters agreed well with dispersoid spacings for the Al alloys, and with grain size for the Ti alloy.

- o Physical events involved in the two-stage (blunting-brittle microfracture), multi-cycle creation of a fatigue striation were interpreted in terms of crack tip fatigue substructure and associated microvoid formation.

D. References

1. D. L. Davidson and J. Lankford, Fatigue Mechanisms: Advances in Quantitative Measurement of Physical Damage, ASTM STP 811, Philadelphia, PA, 1983, 371.

2. J. Lankford and D. L. Davidson, Acta Met., 31, 1983, 1273.

3. D. L. Davidson and J. Lankford, Fat. Eng. Mat. Struct., 6, 1983, 241.

4. S. B. Chakrabortty, Fat. Eng. Mat. Struct., 2, 1979, 331.

5. H. W. Liu and N. Ino, Fracture 1969, Chapman and Hall Ltd, London, 1969, pp. 812-823.

6. J. Lanteigne and J.-P. Bailon, Met. Trans. A, 12A, 1981, 459.

7. A. Saxena and S. D. Antolovich, Met. Trans. A, 6A, 1975, 1809.

8. D. L. Davidson, Scanning Electron Microscopy/1979/II, 1979, 79.

9. D. R. Williams, D. L. Davidson, and J. Lankford, Exp. Mech., 20, 1980, 134.

10. A. Nagy, J. B. Campbell, and D. L. Davidson, Rev. Sci. Instr., 55, 1984, 778.

11. D. L. Davidson and J. Lankford, Fat. Eng. Mat. Struct., 7, 1984, 29.

12. D. L. Davidson, Acta Met., 32, 1984, 707.

13. J. Lankford and D. L. Davidson, Crack Length Measurement II, ed. C. J. Beevers, EMAS, London, 1982, 79.

14. J. P. Hirth and J. Lothe, "Theory of Dislocations", McGraw-Hill Publ. Co., New York, 1968, p. 704.

15. D. L. Davidson and J. Lankford, Mat. Sci. Eng., 74, 1985, 189.

16. D. L. Davidson and J. Lankford, Met. Trans., 15A, 1984, 1931.

17. D. L. Davidson and J. Lankford, High-Strength Powder Metallurgy Aluminum Alloys II, ed. G. J. Hildeman and M. J. Koczak, TMS-AIME, N.Y. (in press).

18. K. J. Nix and H. M. Flower, Acta Met., 30, 1982, 1549.

II. FRACTURE MECHANISMS IN SINGLE CRYSTAL NICKEL-BASE SUPERALLOYS

A. Research Objectives

1. Determine the influence of crystallographic orientation on subcritical crack growth and unstable fracture.

2. Identify the relative importance of shear and normal stresses on slip band cracking.

3. Define the role of slip character on subcritical crack growth and unstable fracture.

4. Develop a model for prediction of fracture behavior.

B. Summary of Research Efforts

Both experimental and theoretical studies were conducted to achieve the program objectives. The experimental efforts involved examining the fatigue crack growth behavior of a Ni-base single crystal alloy as a function of crystallographic orientation, stress state, and slip morphology. The theoretical efforts involved examining the interactions of the crack-tip stress field and slip character, and the conditions that lead to crystallographic cracking.

The material selected for study in this program was the Mar-M200 single crystal alloy. The composition of the material in wt. pct. was: Ni-9Cr-10Co-12.5W-1Nb-4.7Al-1.7Ti. Carbon content was less than 50 ppm. The single crystals were solutionized at 1232 C for four hours and subsequently aged at 871 C for 32 hours. The microstructure consisted of cuboidal γ' in a γ matrix. The size and volume fraction of γ' were 0.35 μm measured on edge and 65%, respectively.

1. Effect of Crystallographic Orientation on Fatigue Crack Growth

High- and low-cycle fatigue studies [1-4] of columnar-grained and single crystal Ni-base superalloys have demonstrated that extended crystallographic cracking on {111} planes, Stage I fatigue [5], can be expected at all cyclic frequencies for temperatures up to ≈760 C and at even higher temperatures for engine excitation frequencies [4]. To develop a fundamental understanding of this fatigue behavior, the effects of crystallographic orientation on the mode of cracking and the crack growth rate in Mar-M200 single crystals were studied. Crack growth tests were performed on compact-tension specimens of seven different orientations at room temperature under load-controlled conditions. The test frequency was 20 Hz, and the applied mininum-to-maximum stress ratio, R, was either 0.1 or 0.5.

All the single crystal compact-tension specimens failed on planes which were inclined to the loading axis as well as to the width and thickness of the specimens. Being inclined to the stress axis, the fatigue cracks were therefore mixed-mode cracks containing Mode I, II, and III components. The

stress intensity factor expression for a Mode I crack in the ASTM Standard would not be applicable for the mixed-mode cracks. One of the contributions of the present effort was developing K solutions for inclined cracks in anisotropic compact-tension specimens [6]. Because of this work, it was possible to analyze the crack growth behavior and the critical stress intensities at overload fracture [6] of Mar-M200 single crystals, despite the complexity of the crack geometry.

An effective stress intensity range, ΔK_{eff}, was developed for correlating crack growth data of anisotropic materials containing mixed-mode cracks. The effective ΔK, defined on the basis of the elastic strain energy release rate, was obtained by summing the squares of individual ΔK components [7,8]. Correlation of effective ΔK and crack growth rate of Mar-M200 single crystals of various crystallographic orientations, shown in Fig. 1, indicated that the crack growth rate was dependent on crystallographic orientation. At a given ΔK, the highest crack growth rate was observed in the [230] orientation, while the slowest crack growth rates were observed in the [111] and [150] oriented specimens.

Two surface analyses were used to identify the fracture planes. On the macroscopic scale, all the single crystal specimens failed by dominant cracks propagating on either a single {111} plane or a combination of {111} planes, which are generally the planes of the highest or second highest resolved shear stress. The dominant cracks, however, also showed a significant amount of crack branching and deflection. Fractographic analyses were performed on the fractured specimens via scanning electron microscopy. The consequence of the tortuous crack paths, as revealed by the fractographic studies, was that the fracture surfaces of the single crystal specimens contained a substantial number of asperities or protrusions as well as black debris which was generally associated with the asperities. The number of fracture surface asperities, ridges, and debris varied with specimen orientation [7]. The largest amount of crack branching and black debris were observed in the [111] and [150] specimens, which also manifested the lowest crack growth rate at a given ΔK_{eff}. Auger spectroscopy was performed on both the metallic part of the fracture surface and the black debris. The result indicated a high oxygen-to-nickel peak ratio in the debris, which persisted after sputtering for two minutes. This suggests that the black debris might represent oxides formed as the result of rubbing of the fracture surface asperities.

The results of this research indicate that the apparent effect of crystallographic orientation on crack growth rate can be attributed to crack deflection, branching, and roughness-induced closure. The consequences of crack branching and deflection in Mar-M200 single crystals are twofold: (1) a direct reduction of local effective ΔK and the driving force for crack growth as the result of crack deflection and branching [9], and (2) rough fracture surfaces containing asperitites which can make contact, rub and introduce roughness-induced closure, and thereby cause a further reduction in the local driving force, i.e., the effective ΔK for crack growth [10]. The black debris observed on the fracture surfaces of some of the single crystals is a manifestation of and direct evidence for roughness-induced closure in this material.

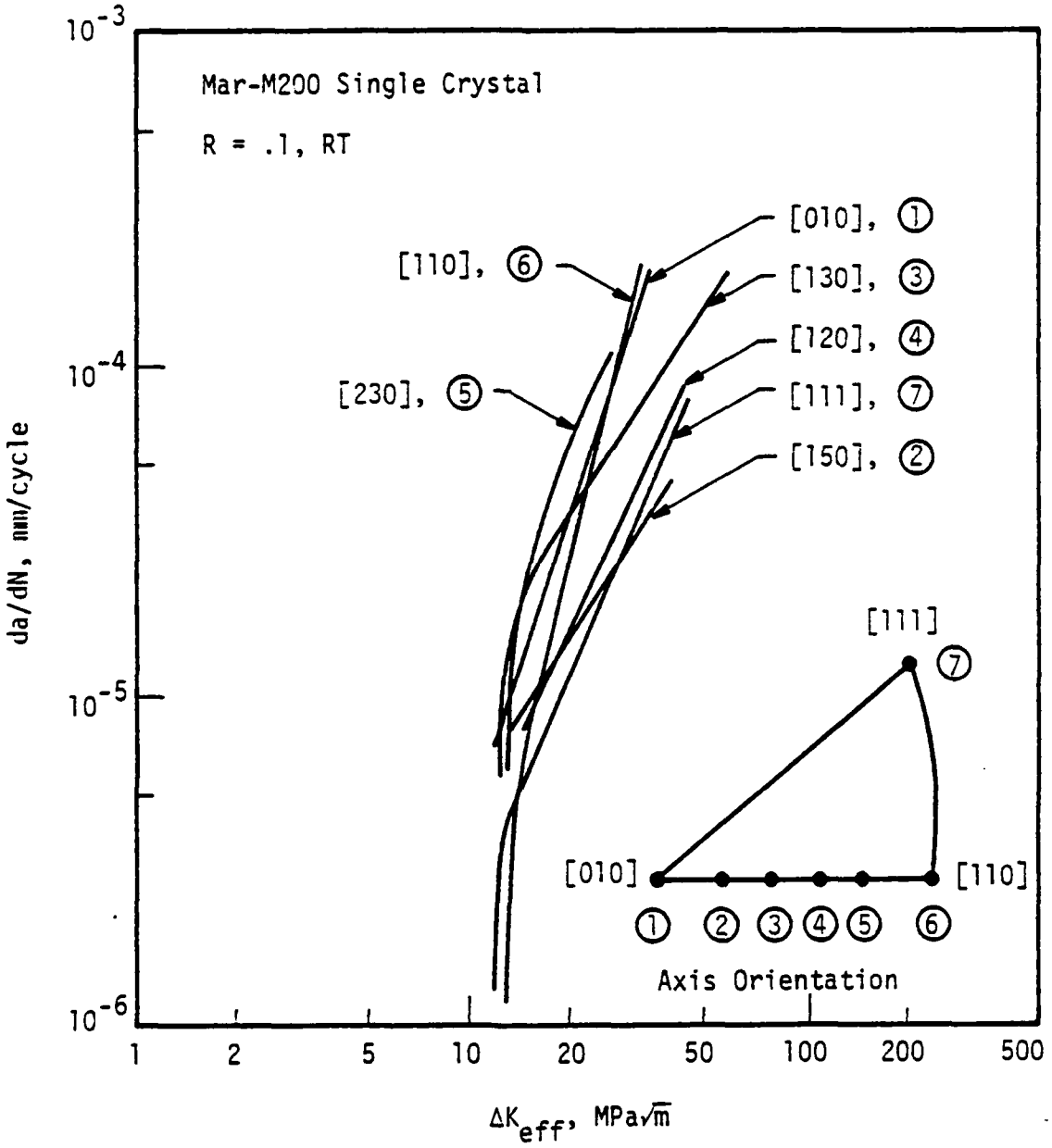

Figure 1. Summary of crack growth rate of Mar-M200 single crystals of various crystallographic orientations as a function of effective stress intensity range. The apparent dependence of crack growth rate on crystallographic orientation is the consequence of crack deflection, branching, and roughness-induced closure.

Out-of-plane secondary slip, which is noncoplanar with the crack, was identified as an important factor in the fatigue crack growth process of Mar-M200 and possibly other Ni-base superalloy single crystals. Significant effects of the out-of-plane secondary slip include: (1) the size of the out-of-plane secondary slip zone determines the normal stress concentration at the crack tip [11-13], and (2) decohesion of the secondary slip bands can cause crack deflection, branching, and potentially roughness-induced crack closure.

2. Effect of Stress State on Cracking Along Slip Bands

Crack growth experiments were performed on [010] and [011] oriented tubular specimens at room temperature in a multiaxial, servo-controlled hydraulic testing machine by applying combined cyclic axial loads and torques under load-controlled conditions. Five different stress states were examined by varying the ratio of the applied shear stress range to axial stress range, $\Delta\tau/\Delta\sigma$. These stress states included pure cyclic tension ($\Delta\tau/\Delta\sigma=0$), fully-reversed torsion ($\Delta\tau/\Delta\sigma=\infty$), and combined cyclic tension and torsion with $\Delta\tau/\Delta\sigma$ ratios of 0.5, 1, and 2. In the multiaxial fatigue cases, the applied torques were fully reversed at a frequency of 5 Hz, while the axial stresses were applied at a frequency of 10 Hz. In all cases involving cyclic axial loads, the minimum to maximum axial stress ratio, R, was 0.1. Crack length was measured using a replication technique.

As in the compact-tension specimens, all but one of the tubular specimens failed on either a single {111} or a combination of {111} planes. The exception was an [010] oriented specimen tested under fully reversed torsion, which failed by propagating a kinked crack part of which was not on a slip plane. Because of mixed-mode loading, the effective ΔK, which as described earlier accounted for mixed-mode cracks and elastic anisotropy, was used for correlating the crack growth data. Another added complexity was that for the inclined cracks, the normal stresses on the crack were compressive during part of the fatigue cycle. As a result, only the normal and shear stress ranges associated with the tensile portion of the fatigue cycle were used for computing the effective ΔK.

Figure 2 shows the correlation of the crack growth data of [010] oriented specimens with effective ΔK without accounting for elastic anisotropy and compressive normal stress in the loading cycle. It indicates a strong dependence of crack growth rate on the applied stress state with the highest growth rate observed under pure tension. On the other hand, this stress state effect is somewhat eliminated when elastic anisotropy and the compressive normal stress on the crack were accounted for in computing the effective ΔK. As illustrated in Fig. 3, the crack growth rates for the $\Delta\tau/\Delta\sigma$ ratios of 0, 0.5 and 1.0 form a small scatter band, indicating the absence of a stress state effect. The lower crack growth rates observed at $\Delta\tau/\Delta\sigma$ ratios of 2.0 and ∞ indicate a stress state dependence which has been identified to arise mainly from roughness-induced closure accompanied by the propagation of branched or kinked cracks [8].

Critical multiaxial crack growth experiments were conducted on tubular specimens of five different combinations of axis and notch orientation and at a $\Delta\tau/\Delta\sigma$ ratio of unity. As shown in Fig. 4, the crack growth rates of

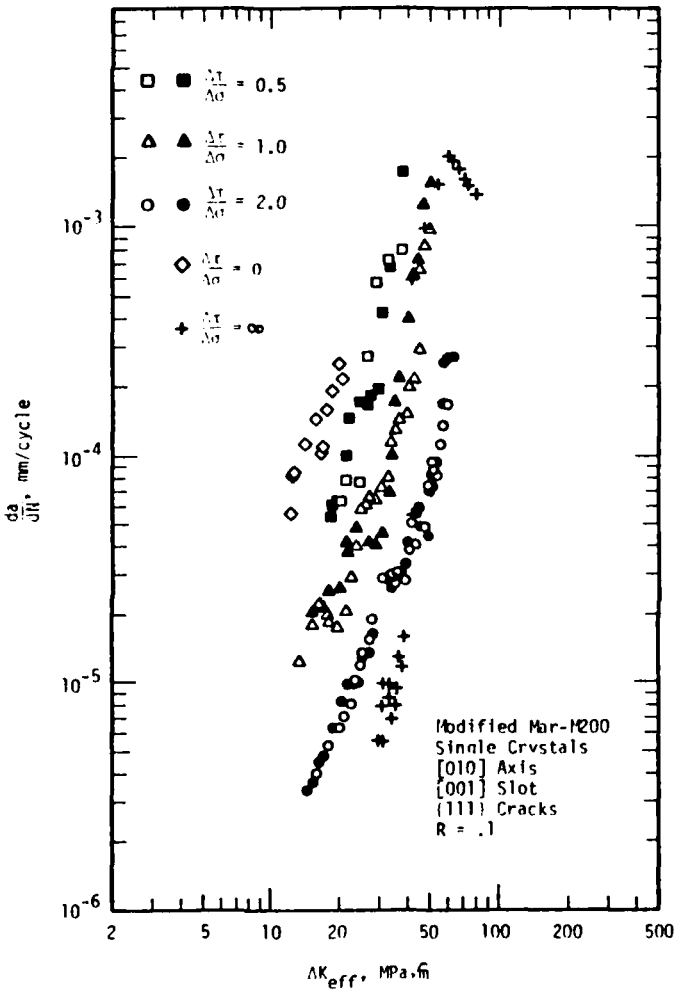

Figure 2. Multiaxial fatigue crack growth rate of [010] oriented Mar-M200 single crystals at various $\Delta\tau/\Delta\sigma$ ratios as a function of an effective stress intensity range without accounting for elastic anisotropy and compressive loads in the fatigue cycles.

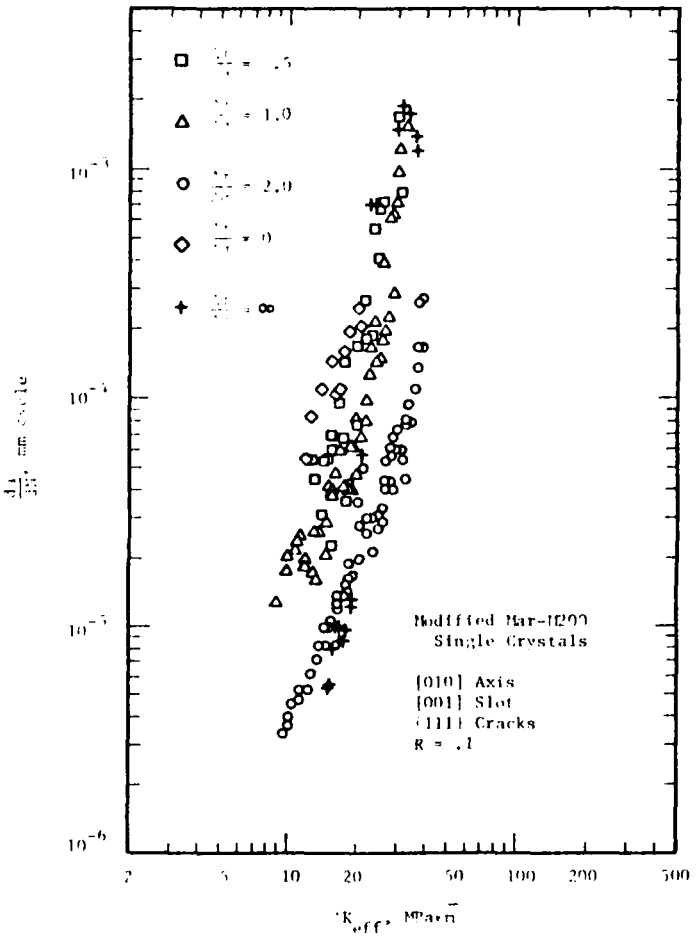

Figure 3. Multiaxial fatigue crack growth rate of [010] oriented Mar-M200 single crystals at various $\Delta\tau/\Delta\sigma$ ratios as a function of an effective stress intensity range that accounts for elastic anisotropy and compressive loads in the fatigue cycles. The apparent dependence of crack growth rate on the applied stress state at $\Delta\tau/\Delta\sigma$ values of 2 and ∞ is the result of roughness-induced crack closure.

these specimens form a small scatter band which is independent of crystallographic orientation.

A very significant conclusion that can be drawn form the crack growth results shown in Figs. 1, 3, and 4 is that in the absence of crack closure, effective ΔK is the driving force for crack growth for both uniaxial and multiaxial fatigue. The crack growth rate, uniquely defined by the ΔK_{eff} parameter, is independent of the applied stress state and crystallographic orientation.

3. The Role of Slip Character in Fatigue Crack Growth

The effect of slip character on crack growth was investigated by testing Mar-M200 single crystal tubular specimens at a temperature regime, 982 C, which is conducive to multiple and homogeneous slip. Conducted on a multiaxial testing machine equipped with an induction heating unit, crack growth tests were performed as a function of crystallographic orientation and the applied stress state, including uniaxial and multiaxial loading. The frequency for the uniaxial fatigue crack growth tests was 10 Hz. In the multiaxial fatigue cases, the applied torques were fully reversed and were, with one exception, in phase with the axial stress at a 10 Hz frequency. In one particular case, out-of-phase loading was used with the shear stress frequency (5 Hz) being half of that for the axial stress (10 Hz). In all cases, the applied R ratio was 0.1. Crack length was measured using a replication technique by cooling the specimens to room temperature.

The [010], [111] and [211] oriented single crystal specimens subjected to uniaxial cyclic loading showed comparable crack growth rates at an equivalent ΔK, suggesting that the effect of crystallographic orientation on crack growth is, at most, minimal. In addition, the [010] and [011] specimens tested at combined tension and torsion at $\Delta\tau/\Delta\sigma$ ratios of 0.5 and 1 also indicated comparable crack growth rates at a given effective ΔK. Since ΔK is equal to effective ΔK for uniaxial loading, the results imply a unique relationship between crack growth rate and effective ΔK, which is indeed the case, as shown in Fig. 5.

Light and scanning electron microscopy were used to study the replicas of the cracked specimens and the fracture surfaces, respectively. Fatigue crack growth in Mar-M200 single crystals at 982 C was generally found to occur in a non-crystallographic manner, i.e., the macroscopic crack planes were not slip planes. For both uniaxial and multiaxial loading, crack growth occurred normal to the principal stress direction and in a direction along which both ΔK_{II} and ΔK_{III} vanished. Consequently, the effective ΔK was reduced to ΔK_I and the rate of crack propagation was controlled by ΔK_I only. Futhermore, fatigue striations were observed on the fracture surfaces of the single crystal specimens, confirming that crack growth at 982 C indeed occurred by Stage II fatigue [5]. The only exception was the [211] specimen which exhibited fracture surface ridges that were covered with striations.

A significant result of this study [14] is the demonstration that cracking along crystallographic slip bands is prohibited at a temperature

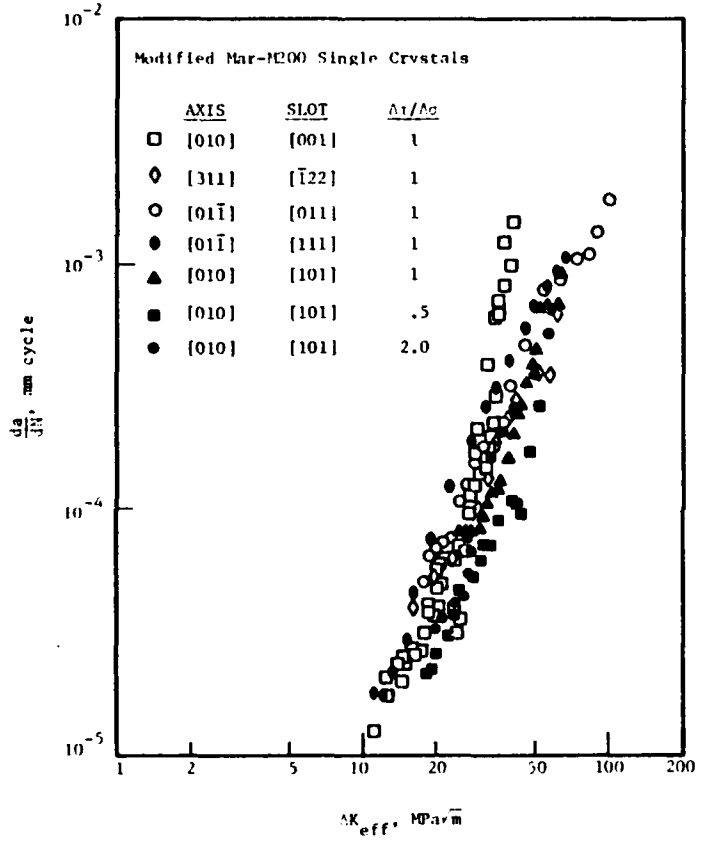

Figure 4. Summary of multiaxial fatigue crack growth rate of Mar-M200 single crystals of various combinations of axis and notch orientations at $\Delta\tau/\Delta\sigma = 1$.

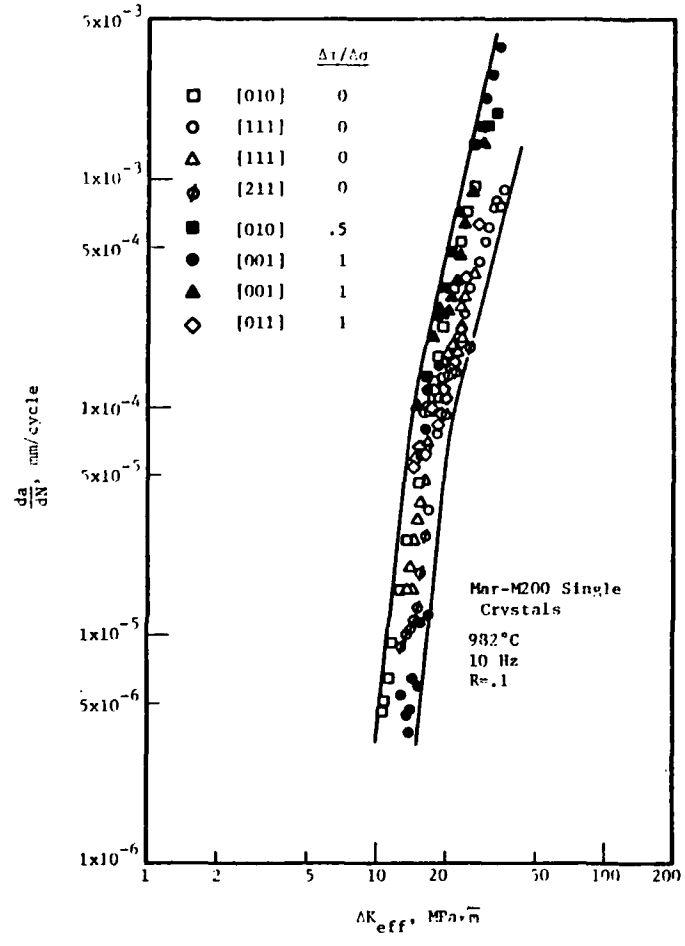

Figure 5. Summary of uniaxial and multiaxial fatigue crack growth rates of Mar-M200 single crystals at 982°C.

where there is a propensity for multiple and homogeneous slip at the crack tip. As will be discussed later, this result provides a critical test of a fracture model [11-13]. Another contribution is the demonstration of the potential use of the effective ΔK for correlating and predicting uniaxial and multiaxial fatigue crack growth data at ambient and elevated temperatures.

4. Fracture Along Coplanar Slip Bands: The Coplanar Slip Model

The experimental results clearly indicate that crystallographic cracking along a single or a combination of {111} slip planes is a predominant fracture mode in Mar-M200 single crystals at ambient temperature. According to the coplanar slip model proposed by Koss and Chan [11,12], this fracture behavior can be explained on the basis of the inability of coplanar slip to relax the normal stress components ahead of the crack, creating an elastic-plastic stress state which is not conducive to out-of-plane noncoplanar secondary slip. The coplanar slip model was extended in this research to consider cracking along coplanar slip bands in the presence of cross slip. The result indicates that cross slip would not be effective in relaxing the normal stresses at the crack tip. Dictated by the crack-tip elastic singularity, the normal stress components continue to increase up to very close to the crack tip, and can be relaxed by out-of-plane, noncoplanar secondary slip only. This leads to a buildup of normal stress on the coplanar slip bands, which can be quite high as shown by calculations conducted in this study. Figs. 6a-c illustrate that for a 45° mixed Mode I and II crack, the maximum normal stress, σ^{m}_{YY} at the secondary slip plastic zone can exceed 1.4 σ_Y, where σ_Y is the yield stress.

The presence of large normal and shear stresses on the coplanar slip bands help explain: (1) the tendency of the fatigue crack to continue propagating along the {111} plane, (2) the cleavage-like fracture appearance associated with coplanar slip band cracking, and (3) simultaneous cracking on two cross-slip {111} planes leading to the formation of fracture surface ridges observed in Mar-M200 single crystals [7,8,13].

The theoretical efforts also identified out-of-plane noncoplanar slip as an important factor in controlling crack growth along coplanar slip bands. In particular, the magnitude of the normal stress at the crack tip is dictated by the size of the nonplanar secondary slip plastic zone. In addition, decohesion of the secondary slip planes can lead to crack branching, deflection and potential roughness-induced crack closure.

The buildup of normal stress on the coplanar crack is obviously very sensitive to the activation of out-of-plane noncoplanar secondary slip. There is considerable evidence in the literature which indicates that cube slip is operative in Mar-M200 single crystals at temperatures above 800 C [15-17]. The effects of cube slip are to lower the apparent critical resolved shear stress, and to produce a more isotropic deformation behavior [15,16]. Because of the increased number of slip systems in Mar-M200 single crystals at 982 C, crack tip deformation is likely to be more homogeneous due to the propensity for multiple slip. Under this circumstance, an incipient coplanar crack along a {111} slip band is difficult to develop because any normal stress buildup on

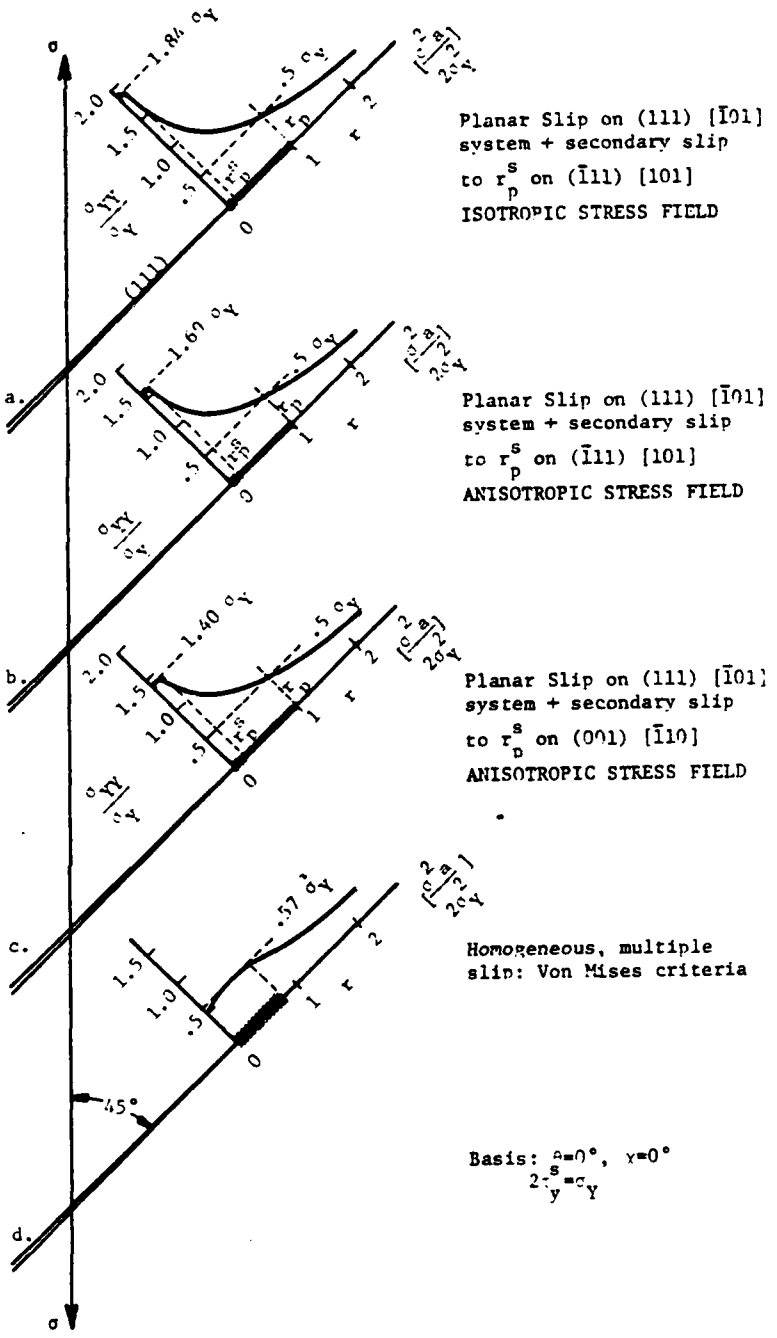

Figure 6. Stress distributions ahead of a mixed-Mode I and II crack that is inclined at 45° to the loading axis as a function of slip character at the crack tip. These stress distributions were computed based on the coplanar slip model.

the coplanar slip band can be readily relaxed by noncoplanar secondary slip. Furthermore, dislocations on the incipient slip bands are also easily dispersed due to the propensity for dislocation climb at this temperature [18]. The normal stress distribution ahead of a crack in a homogeneous, multiple slip material, i.e., a continuum material, was calculated and shown in Fig. 6d. Note that the value of the maximum normal stress, σ^m_{YY}, for the multiple slip material at the crack tip is considerably lower ($\sigma^m_{YY}=.57\sigma_Y$) than that for single crystals exhibiting secondary slip on an individual slip system ($\sigma^m_{YY} > 1.4\sigma_Y$). These results suggest that the difference in the cracking behavior observed in Mar-M200 single crystals at 25 and 982 C can be attributed to crack-tip slip morphology in general and the activation of homogeneous multiple slip at 982 C in particular.

C. Accomplishments

1. The dependence of crack growth rate on crystallographic orientation observed in Mar-M200 single crystals was shown to be an effect that arises from crack deflection, branching, and roughness-induced crack closure.

2. The stress-state dependence of crack growth rate in Mar-M200 single crystals was determined to arise from roughness-induced crack closure associated with the propagation of branched and kinked cracks under predominantly shear loading.

3. An effective stress intensity range parameter was developed for correlating crack growth data of ansiotropic materials containing mixed-mode cracks. It was shown that in the absence of roughness-induced crack closure, the effective ΔK represents the driving force for fatigue crack growth under both uniaxial and multiaxial loading at ambient and elevated temperatures. The crack growth rate, uniquely defined by the ΔK_{eff} parameter, is independent of the applied stress state and crystallographic orientation.

4. Crystallographic cracking along a single {111} or a combination of {111} planes was shown to be the predominant fracture mechanism in Mar-M200 single crystals at ambient temperature. This fracture mode was prohibited at an elevated temperature regime where there was propensity for homogeneous multiple slip.

5. A fracture model was extended to examine the conditions that lead to crystallographic cracking along slip bands in the presence of cross and secondary slip. The results show that whether or not crystallographic cracking occurs depends on the normal stress on the incipient coplanar slip bands. The normal stress buildup ahead of a fatigue crack is dependent on the crack tip slip character and controlled by noncoplanar secondary slip.

6. Elevated-temperature multiaxial fatigue crack growth in Mar-M200 single crystals was shown to occur normal to the principal stress direction and in a direction along which both ΔK_{II} and ΔK_{III} vanished. The crack growth rate was therefore controlled by ΔK_I only.

7. Stress intensity solutions were developed for anisotropic compact-tension specimens containing inclined cracks.

D. References

1. M. Gell and G. R. Leverant, Trans. AIME, 242, 1968, 1869.

2. G. R. Leverant and M. Gell, Trans. AIME, Vol. 245, 1969, 1167.

3. G. R. Leverant and M. Gell, Met. Trans. A, 6A, 1975, 367.

4. D. L. Anton, Acta Met., 32, 1984, 1669.

5. P. J. E. Forsyth, Proc. of the Crack Propagation Symposium, Cranfield, 1961, p. 76.

6. K. S. Chan and T. A. Cruse, Engineering Fracture Mechanics, 1986 (in press).

7. K. S. Chan, J. E. Hack, and G. R. Leverant, "Fatigue Crack Growth in Mar-M200 Single Crystals," Met. Trans. A, 1986 (submitted).

8. K. S. Chan, J. E. Hack, and G. R. Leverant, "Fatigue Crack Propagation in Ni-Based Superalloy Single Crystals Under Multiaxial Cyclic Loads," Met. Trans. A, 1985 (submitted).

9. S. Suresh, Met. Trans., 16A, 1985, 249.

10. S. Suresh and R. O. Ritchie, Met. Trans., 13A, 1982, 1627.

11. D. A. Koss and K. S. Chan, Acta Met., 28, 1980, 1245.

12. D. A. Koss and K. S. Chan, in Dislocation Modeling of Physical Systems, Pergamon Press, 1981, p. 18.

13. K. S. Chan, "Effect of Cross Slip on Crystallographic Cracking in Anisotropic Single Crystals," Acta Met., 1986 (submitted).

14. K. S. Chan and G. R. Leverant, "Elevated-Temperature Crack Growth Behavior of Mar-M200 Single Crystals," Met. Trans A, 1986 (submitted).

15. B. H. Kear and B. J. Piearcey, Trans. AIME, 239, 1967, 1209.

16. S. M. Copley, B. H. Kear, and G. M. Rowe, Mater. Sci. Eng., 10, 1972, 87.

17. A. F. Giamei, "Deformation and Fracture of Advanced Anisotropic Superalloys," Final Technical Report, Contract No. F44620-76-C-0028, Air Force Office of Scientific Research, 1979.

18. M. Gell and G. R. Leverant, Fatigue at Elevated Temperatures, ASTM STP 520, ASTM, 1973, p. 37.

III. PUBLICATIONS

A. Task 1. Influence of Metallurgical Structure Upon Crack Tip Micromechanics

1. "Experimental Mechanics and Modeling of Fatigue Crack Growth", D. L. Davidson, Proceedings of Modelling Problems in Crack Tip Mechanics, Martinus Nijhoff Publishers BV, 217, 1984.

2. "A Model for Fatigue Crack Advance Based on Crack Tip Metallurgical and Mechanics Parameters", D. L. Davidson, Acta Metallurgica, 32, 707, 1984.

3. "Fatigue Crack Growth Mechanics of Ti-6Al-4V in Vacuum and Humid Air", D. L. Davidson and J. Lankford, Metallurgical Transactions, 15A, 1931, 1984.

4. "Experimental Characterization of Fatigue Crack Tip Processes", J. Lankford and G. R. Leverant, Proceedings of the Eighth Inter-American Conference on Materials Technology, 7-7, 1984.

5. "Fatigue Crack Tip Mechanics of a Powder Metallurgy Aluminum Alloy in Vacuum and Humid Air", D. L. Davidson and J. Lankford, Fatigue of Engineering Materials and Structures, 7, 29, 1984.

6. "Experimental Mechanics of Fatigue Crack Growth: The Effect of Crack Size", D. L. Davidson and J. Lankford, Fundamentals of Deformation and Fracture, Ed. B. A. Bilby, K. J. Miller, and J. R. Willis, Cambridge University Press, Cambridge, England, 529, 1985.

7. "The Effects of Aluminum Alloy Microstructure on Fatigue Crack Growth", D. L. Davidson and J. Lankford, Materials Science and Engineering, 74, 189, 1985.

8. "The Breakdown of Crack Tip Microstructure During Fatigue Crack Extension in Aluminum Alloys", D. L. Davidson and J. Lankford, High-Strength Powder Metallurgy Aluminum Alloys II, Ed. G. J. Hildeman and M. J. Koczak, TMS-AIME, Warrendale, PA, 1986 (in press).

9. "The Distribution of Strain Within Crack Tip Plastic Zones", D. L. Davidson, Engineering Fracture Mechanics, 1986 (in press).

B. Task 2. Fracture Mechanisms in Single Crystal Nickel-Base Superalloys

1. "Fatigue Crack Propagation in Ni-Based Superalloy Single Crystals Under Multiaxial Cyclic Loads", K. S. Chan, J. E. Hack, and G. R. Leverant, submitted to Metallurgical Transactions, 1985.

2. "The Stress Intensity Factors for Anisotropic Compact-Tension Specimens with Inclined Cracks", K. S. Chan and T. A. Cruse, Engineering Fracture Mechanics, 1986 (in press).

3. "Fatigue Crack Growth in Mar-M200 Single Crystals", K. S. Chan, J. E. Hack, and G. R. Leverant, Metallurgical Transactions A, 1986 (submitted).

4. "Effect of Cross-Slip on Crystallographic Cracking in Anisotropic Single Crystals", K. S. Chan, Acta Metallurgica, 1986 (submitted).

5. "Elevated-Temperature Fatigue Crack Growth Behavior of Mar-M200 Single Crystals", K. S. Chan and G. R. Leverant, Metallurgical Transactions A, 1986 (submitted).

IV. PROGRAM PERSONNEL

Name	Title	
Dr. James Lankford	Institute Scientist	Co-Principal Investigators
Dr. David L. Davidson	Institute Scientist	
Dr. Gerald R. Leverant	Director, Materials Sciences	
Dr. Kwai S. Chan	Senior Research Engineer	
Dr. John Hack	Senior Research Engineer	
Mr. John Campbell	Senior Technician	
Mr. Harold Saldana	Senior Technician	
Mr. James Spencer	Senior Technician	
Mr. Forrest Campbell	Staff Technician	
Mr. Kyle Short	Senior Technician	